An Improved Inter-Relay Cooperation Scheme for Distributed Relaying Networks

Meng Wu*, Wenyao Xue†, Dirk Wübben*, Armin Dekorsy*, and Steffen Paul†
*Department of Communications Engineering, University of Bremen, 28359 Bremen, Germany
Email: {wu, wuebben, dekorsy}@ant.uni-bremen.de
†Department of Communication Electronics, University of Bremen, 28359 Bremen, Germany
Email: {xue, steffen.paul}@me.uni-bremen.de

***Abstract*—We consider a two-hop distributed relaying network using orthogonal space-time block codes (OSTBC), where several relays using Decode-Forward (DF) support the transmission from one source to one destination. In order to mitigate the impact of error propagation for DF, an inter-relay cooperation (IRC) scheme allowing message exchanges among the relays was presented in our previous work based on punctured channel codes. Specifically, one of the relays that decodes the source message correctly re-generates and broadcasts the punctured bits as side information to support the relays with decoding errors for re-decoding. Subsequently, only the error-free relays transmit to the destination using OSTBC. It was shown that this IRC scheme may increase the number of error-free relays when at least one relay decodes the source message correctly.**

In this paper we focus on the scenario that all relays fail to decode the source message correctly. To this end, an improved IRC scheme is presented based on received signal exchange, in which the whole or part of the received frame are exchanged among the relays to apply signal combining. Additionally, the total energy consumption for signal transmission, baseband processing and RF circuit at all relays is evaluated for practical preferences. It is shown that the improved scheme outperforms our original scheme significantly with respect to the overall system throughput.

I. Introduction

The concept of cooperation attracts great interests in bringing diversity gains that combat fading effectively in wireless communications [1]. By introducing relaying nodes, the source-destination link is expanded with improved performance. Furthermore, by clustering several relaying nodes to a virtual antenna array (VAA), coding and signal processing approaches known for multiple antenna systems can be applied in such distributed networks. In [2] Laneman *et al.* investigated a distributed relaying network with single-antenna relays using Decode-Forward (DF). By exploiting cyclic redundancy check (CRC) codes, the relays that decode the source message correctly ("correct relays") transmit to the destination using orthogonal space-time block codes (OSTBC). However, if all relays encounter decoding errors ("erroneous relays"), the relays are deactivated and the destination decodes the source message only assuming the presence of the direct link. It was demonstrated, that the diversity degree depends on the number of cooperating terminals, but not on the number of correct relays. Note that due to the distributed nature of the network, the transmitting relays have to be well synchronized, which results in extra overhead [3]. A simple but effective approach to avoid extra synchronization effort is given by relay selection for transmission, e.g., Nosratinia *et al.* investigated a relay selection scheme [4], [5] in which only the correct relay with the highest instantaneous signal-to-noise ratio (SNR) on the relay-destination link transmits to the destination.

In our previous work [6] a distributed relaying system is considered without the presence of the direct source-destination link due to its large distance. In order to mitigate the impact of error propagation for DF, an inter-relay cooperation (IRC) scheme has been presented that allows message exchanges within the VAA. Specifically, by using a punctured channel code at the source, if at least one but not all relays decode the source message correctly, the bits punctured at the source are re-generated and exchanged from one of the correct relays to the erroneous relays in the IRC phase for re-decoding. Therefore, the number of correct relays may be increased, which transmit to the destination using OSTBCs.

In this work we concentrate on the information exchange for IRC when all relays are erroneous. In this case, we present an improved IRC scheme based on received signal exchange. By exchanging the whole or part of the received frame within the VAA, signal combining strategies can be applied at the relays. Another contribution of this paper is the consideration of energy consumption for signal transmission, baseband processing and RF circuit for practical preferences. The system performance is evaluated based on a throughput analysis with respect to the total energy consumption.

The remainder of this paper is organized as follows. The distributed relaying system is described in Section II. The IRC scheme based on punctured channel codes presented [6] is reviewed in Section III. The improved scheme based on the exchange of received signals at the relays is illustrated in detail in Section IV. Section V discusses the energy model at the relays for the improved IRC scheme. Performance evaluations based on the throughput analysis with respect to the total energy consumption are presented in Section VI and Section VII concludes this paper.

II. System Description

We consider a distributed relaying system where one source S communicates with one destination D supported by K relays R_k, $1 \leq k \leq K$, using DF as shown in Fig. 1. All involved nodes are equipped with a single antenna. The relays are clustered

978-1-4577-1924-0/12/$26.00 ©2012 IEEE

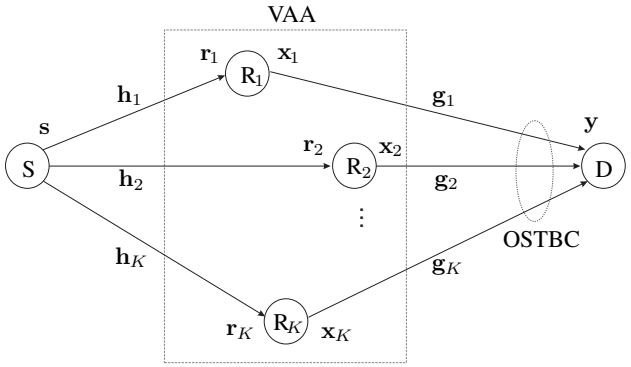

Fig. 1. Distributed relaying system with K relays constituting a VAA. In case of no IRC, all relays participate in the transmission to D using STBC.

to form a VAA operating in half-duplex mode. The network topology is assumed to be fixed, such that each relay R_k knows its own index k. Furthermore, coded Orthogonal Frequency Division Multiplexing (OFDM) technology is applied to the source-relay (SR) and the relay-destination (RD) links to combat multi-path effects. At S the encoded and interleaved code bit vector $\mathbf{c}$ with code rate R_{C} is mapped to N_{FFT} symbols using M-QAM modulation, where N_{FFT} indicates the number of subcarriers. Thus, each OFDM frame contains one complete codeword. Denoting s_m the transmit symbol on subcarrier $1 \leq m \leq N_{\mathrm{FFT}}$, the corresponding received signal $r_{k,m}$ at R_k on subcarrier m can be written as

$$r_{k,m} = h_{k,m} s_m + n_{k,m} \ . \tag{1}$$

The received signal vector $\mathbf{r}_k = [r_{k,1}, r_{k,2}, \cdots, r_{k,N_{\mathrm{FFT}}}]^T$ is decoded to estimate the source message at relay R_k. Subsequently, the re-generated symbol vector $\mathbf{x}_k = [x_{k,1}, x_{k,2}, \cdots, x_{k,N_{\mathrm{FFT}}}]^T$ is transmitted to D in the second phase using an OSTBC. This yields the received signal y_m on subcarrier m at destination D

$$y_m = \sum_{k=1}^{K} g_{k,m} x_{k,m} + q_m \ . \tag{2}$$

The received signal vector $\mathbf{y} = [y_1, y_2, \cdots, y_{N_{\mathrm{FFT}}}]^T$ is linearly combined for STBC detection at the destination. Subsequently, the source message is estimated by decoding. Noticeably, more than 2 transmit antennas ($K > 2$) lead to a rate loss R_{STBC} for OSTBC. In order to achieve the same data rate, we apply rate matching by adapting the channel code rate of the RD link to $R_{\mathrm{C,RD}} > R_{\mathrm{C}}$, such that $R_{\mathrm{STBC}} R_{\mathrm{C,RD}} = R_{\mathrm{C}}$ holds.

In this paper all SR and RD links are assumed to be multi-path Rayleigh block fading and contain N_{H} equal power channel taps in time domain. The corresponding channel coefficients $h_{k,m}$ in (1) and $g_{k,m}$ in (2) on subcarrier m in frequency domain have variance $\sigma_{\mathrm{H}}^2 = 1/(N_{\mathrm{H}} d^{\alpha})$. Here α denotes the path-loss exponent and $d \in \{d_{\mathrm{SR}}, d_{\mathrm{RD}}\}$ represent the distance for the SR and the RD links. Since the relays are assumed to be close to each other, $d_{\mathrm{IRC}} \ll d$ holds with d_{IRC} denoting the distance between the relays. The additive white Gaussian noise (AWGN) terms $n_{k,m}$ and q_m are i.i.d. zero-mean complex random variables with variance σ_n^2. The transmit power at the source S and the VAA are denoted as $\mathcal{P}_{\mathrm{S}}$ and $\mathcal{P}_{\mathrm{R}}$, respectively, where $\mathcal{P}_{\mathrm{R}}$ is equally assigned to the active relays. Furthermore, the power on each node that transmits is equally allocated to the N_{FFT} subcarriers.

III. IRC based on Punctured Channel Codes

In case of no IRC as shown in Fig. 1, all relays transmit to the destination using OSTBC irrespective of the decoding status at the relays. However, if there are relays that failed to decode the source message correctly, decoding errors will be forwarded to the destination, causing error propagation that jeopardizes the overall performance tremendously. In order to mitigate this problem, an IRC scheme based on punctured channel codes was presented in [6] and is reviewed subsequently.

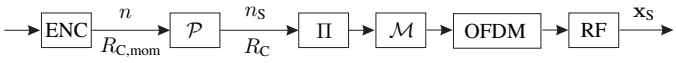

Fig. 2. Block diagram at the source S by using a punctured channel code with n_{pun} punctured bits.

As shown by the block digram at S in Fig. 2, the information bits are encoded by a channel code of mother rate $R_{\mathrm{C,mom}}$ to yield a codeword of length n. Afterwards, n_{pun} bits are punctured, resulting in a shortened codeword of length $n_{\mathrm{S}} = n - n_{\mathrm{pun}}$ and code rate R_{C}. The code bit vector after puncturing is interleaved and modulated to yield the OFDM frame $\mathbf{x}_{\mathrm{S}}$ for transmission.

After receiving and decoding, each relay R_k is aware of its own decoding status by using a CRC code with perfect error detection and negligible overhead. The relays now interchange a one-bit acknowledgement (ACK) or negative acknowledgement (NAK) denoted as CRC bit. Due to the fixed structure of the network, the CRC bits can be sent in a pre-fixed order to avoid index overhead. Consequently, all relays are aware of the set $\mathcal{D}$ containing all correct relays. Depending on the cardinality $|\mathcal{D}|$ three events can be distinguished.

- **Event $\mathbf{E}_1$:** $|\mathcal{D}| = K \rightarrow$ **all relays correct**
  An exchange of punctured bits is not necessary since all relays have decoded the source message without errors. Therefore, K relays transmit to D using OSTBC.
- **Event $\mathbf{E}_2$:** $|\mathcal{D}| = 0 \ \rightarrow$ **all relays erroneous**
  One possibility could be switching to Amplify-Forward (AF) but is not considered here, i.e., DF is still used and K relays transmit to D using OSTBC.
- **Event $\mathbf{E}_3$:** $1 \leq |\mathcal{D}| < K \rightarrow$ **some relays correct**
  One relay in $\mathcal{D}$ generates and broadcasts $n_{\mathrm{IRC}} \leq n_{\mathrm{pun}}$ punctured bits. The erroneous relays combine the source message with these punctured bits for re-decoding. Subsequently, the erroneous relays broadcast their CRC status again to determine the new set $\mathcal{D}'$. Finally, the relays in $\mathcal{D}'$ transmit to destination D using OSTBC.

This IRC scheme may increase the number of correct relays when event E_3 occurs, i.e., $|\mathcal{D}'| \geq |\mathcal{D}|$. Correspondingly, the

system equation (2) for the transmission from the VAA to D on subcarrier m is re-formulated as

$$y_m = \sum_{k \in \mathcal{D}'} g_{k,m} x_{k,m} + q_m \tag{3}$$

for E_3. It should also be emphasized that $n_{\text{IRC}} \leq n_{\text{pun}}$ holds in E_3, indicating that it is possible to exchange only part of the punctured bits in the IRC phase. Exchanging less punctured bits leads to smaller amount of overhead but results in worse re-decoding quality. This trade-off has been observed and examined in [6], which implies that the number of exchanged punctured bits n_{pun} needs to be chosen appropriately.

IV. IRC BASED ON RECEIVED SIGNALS

Based on punctured channel codes, the IRC scheme in Section III may increase the number of correct relays in E_3 when at least one relay is able to decode the source message correctly. However, when E_2 occurs, i.e., all relays have decoding errors, the punctured bit may not be correctly generated. To this end, we present in this paper an improved IRC scheme based on the exchange of received signals. Depending on the amount of exchanged received signals, signal combining is applied on different subcarriers at the relays.

A. Full Exchange of Received Signals

In case of full exchange of received signals, the whole received OFDM frames at the relays are shared with each other in the VAA, leading to an overhead of $\Phi_{\text{IRC}} = KN_{\text{FFT}}$ complex symbols to be exchanged. By applying maximum ratio combining (MRC) at each relay based on full exchange of received signals, the combined signal on subcarrier m at relay R_k is written as

$$r_{\text{full},k,m} = \sum_{j=1}^{K} h_{j,m}^* r_{j,m} \tag{4}$$

assuming that the signal $r_{j,m}$, $\forall j, j \neq k$ from relay R_j is perfectly received at R_k. Note that throughout this paper, the relays are assumed to be close to each other and the inter-relays channels are subject to AWGN noise n_{IRC} only with high received SNR. Therefore, the noise term n_{IRC} is neglected for the analog transmission of received signals.

B. Partial Exchange of Received Signals

In order to reduce the cooperation overhead, only part of the received signals are shared between the relays. To this end, the part of received signals to be exchanged should be selected properly. In [7], [8] a generalized selection combining (GSC) strategy was investigated that combines the received signals or the log-likelihood ratios (LLR) from some of the communication links for single-input single-output (SIMO) systems. This combining strategy can be applied at the distributed relays with decreased amount of exchanged information compared to full signal exchange. We define first the relay index κ_m as

$$\kappa_m = \arg\max_k \{|h_{k,m}|^2\} , \tag{5}$$

with $|h_{k,m}|^2$ proportional to the instantaneous SNR_{SR} on subcarrier m. Furthermore, the vector corresponding to the highest SNR_{SR} is defined as

$$\hat{\mathbf{h}} = [|h_{\kappa_1,1}|^2, |h_{\kappa_2,2}|^2, ..., |h_{\kappa_{N_{\text{FFT}}},N_{\text{FFT}}}|^2] \tag{6}$$

based on the subcarrierwise selected relay (5). Subsequently, $\hat{\mathbf{h}}$ is sorted in decreasing order, yielding the sorted vector $\hat{\mathbf{h}}_{\text{s}}$, where $\hat{h}_{\text{s},m} > \hat{h}_{\text{s},m+1}$, $\forall m$, $m \neq N_{\text{FFT}}$. For partial exchange, only the subcarriers with respect to the first λN_{FFT} terms in $\hat{\mathbf{h}}_{\text{s}}$ are selected for received signal exchange, where λ denotes a proportion factor in the range $0 < \lambda \leq 1$. Note that for the selected subcarriers, only one relay with index κ_m transmits the corresponding received signal. Therefore, the overhead is reduced to $\Phi_{\text{IRC}} = \lambda N_{\text{FFT}}$. Correspondingly, the combined signal at relay R_k reads

$$r_{\text{partial},k,m} = h_{k,m}^* r_{k,m} + h_{\kappa_m,m}^* r_{\kappa_m,m} \tag{7}$$

assuming perfect exchange for the signal $r_{\kappa_m,m}$. The combining strategy (7) guarantees that the subcarrierwise signal with the highest SNR_{SR} is always involved. Note that R_{κ_m} gets no exchanged received signals on subcarrier m since only one relay exchanges the received signal for each subcarrier.

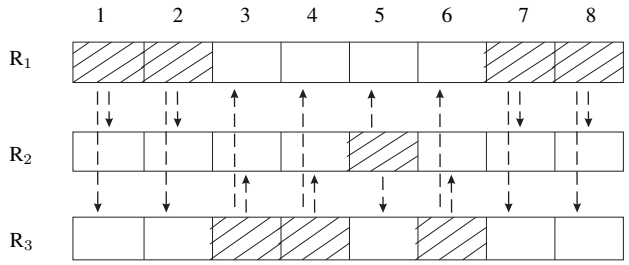

Fig. 3. Am example for the received signal exchange based on subcarrierwise relay selection in E_2 with $K = 3$, $N_{\text{FFT}} = 8$ and $\lambda = 1$. The shadowed subcarriers are those with the highest instantaneous SNR_{SR} among the relays and are selected for received signal exchange.

Fig. 3 illustrates the scheme with partial exchange of received signals for $K = 3$ relays, $N_{\text{FFT}} = 8$ subcarriers and $\lambda = 1$ as an example. The subcarriers 1, 2, 7, 8 at R_1 have the highest SNR_{SR} and thus the corresponding received signals on these subcarriers are exchanged to R_2 and R_3. Similarly, R_2 exchanges its received signal on subcarrier 5 and the received signals on subcarriers 3, 5, 6 are exchanged at R_3.

C. Exchange of Channel State Information (CSI)

In order to apply the presented cooperation schemes in this section, the relays need to share the CSI of the SR links for both subcarrierwise relay selection and signal combining. This requires extra overhead and should be considered adequately. Suppose each relay knows its CSI of the SR link perfectly, which consists of N_{H} complex symbols in time domain, exchanging the CSI among all relays leads to an overhead of $\Phi_{\text{CH}} = KN_{\text{H}}$. Furthermore, it is assumed that all channels are block fading and stay invariant for L OFDM frames, during

which the channel coefficients need to be exchanged only once. Therefore, the data rate is decreased by a factor

$$\rho = \frac{L\Phi_{\text{IRC}}}{L\Phi_{\text{IRC}} + \Phi_{\text{CH}}} \tag{8}$$

for IRC in E_2. Clearly, this effect becomes negligible with growing L. Note that when the energy consumption for baseband processing is considered, $K(K-1)$ extra FFTs are required to obtain the channel coefficients in frequency domain used for the presented combining strategies.

D. Quantization of Received Signals

Practically, analog signals to be exchanged in Subsections IV-A and IV-B need to be quantized before transmitting. The block diagram for bit quantization at a relay that exchanges received signals to others is shown in Fig. 4. The real part and imaginary part of the received signal $r_{j,m}$ to be exchanged are quantized separately by a linear quantizer $\mathcal{Q}$ with Q quantization levels [9] causing the quantization noise n_{Q}. Subsequently, the quantized bits are serially aligned and modulated by M_{IRC}-QAM being used for inter-relay communications.

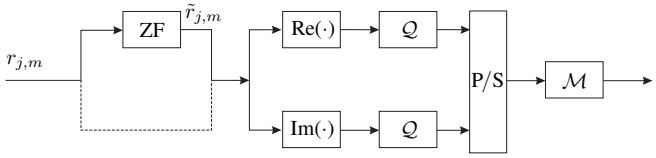

Fig. 4. Block diagram for quantization of the received signals with the application of a ZF equalizer before quantization. As an alternative, the dashed line shows the quantization process without ZF.

Two possibilities for bit quantization are shown in Fig. 4. For the solid line the received signal $r_{j,m}$ to be exchanged is firstly de-rotated using a zero forcing (ZF) equalizer, yielding $\tilde{r}_{j,m}$ before quantization

$$\tilde{r}_{j,m} = \frac{r_{j,m}}{h_{j,m}} = s_m + \frac{n_{j,m}}{h_{j,m}} \,. \tag{9}$$

An alternative is shown by the dashed line, where $r_{j,m}$ is directly quantized without ZF equalization. In this case, the quantization noise n_{Q} is amplified by de-rotating the signal after de-quantization, leading to degraded performance.

As an example we consider the scenario that all $K = 4$ relays fail to decode the source message correctly and partial exchange of received signals with $\lambda = 1/2$ is performed. IRC is only subject to AWGN disturbance with 256-QAM. Denoting p the probability that an erroneous relay is correctly re-decoded after signal combining, Fig. 5 shows the relation between p and SNR_{IRC}. It can be observed that the analog transmission without quantization achieves the best performance. When $Q = 16$ bits are used to quantize the real part or imaginary part of each complex symbol, both schemes with and without ZF approach the analog transmission at high SNR_{IRC} because of small quantization noise n_{Q}. The scheme without ZF leads to significantly degraded performance when $Q = 4$ due to the amplification of n_{Q} by de-rotation. However, de-rotating the signal by ZF before quantization avoids this

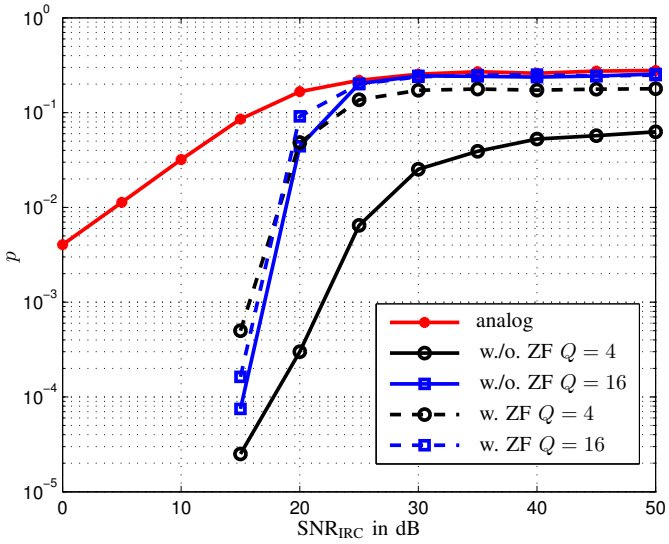

Fig. 5. Probability of correct re-decoding at erroneous relays for received signal exchange with bit-level quantization, $\text{SNR}_{\text{SR}} = 12\,\text{dB}$.

problem and approaches the analog transmission with only a slightly degraded performance. Noticeably, using $Q = 4$ and $M_{\text{IRC}} = 256$ in case of quantization achieves the same overhead as analog transmission, as one analog signal results in one digitally modulated symbol. However, using quantization leads to a more realistic scenario in the implementation perspective. It can also be observed in Fig. 5 that analog transmission achieves much better performance with decreasing SNR_{IRC} since in case of bit quantization one bit error for the inter-relay transmission may result in completely corrupted signal after de-quantization. The performance at lower SNR_{IRC} can be improved by applying a symbol quantizer that quantizes the received signal in symbol level. However, we consider only good inter-relay channels in the sequel, e.g., $\text{SNR}_{\text{IRC}} = 30\,\text{dB}$. Therefore, a bit quantizer as shown in Fig. 4 is still used.

E. Throughput Analysis

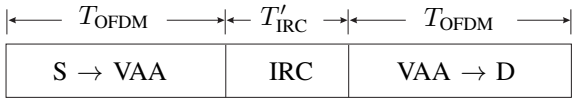

Fig. 6. Transmission timeline for one OFDM frame from S to D via VAA with the extension of IRC that requires a dedicated time slot of duration T'_{IRC}.

Compared to the benchmark system in Fig. 1, IRC consumes extra physical resources. Similar to [6], a dedicated time slot is assigned to IRC, as shown in Fig. 6 for the transmission timeline. Contrary to one OFDM frame duration T_{OFDM} consumed for the SR link and the RD link transmission, T_{s} denotes one symbol duration for the single-carrier transmission in the IRC phase. Thus, the time duration for exchanging the received signals plus the channel coefficients in E_2 is given by

$$T_{\text{rec}} = \left\lceil \frac{2Q\Phi_{\text{IRC}}/\rho}{M_{\text{IRC}}} \right\rceil T_{\text{s}} \,. \tag{10}$$

On the other hand, the required time duration when the punctured bits are exchanged in E_3 is calculated as

$$T_{\text{pun}} = \left\lceil \frac{n_{\text{IRC}}}{M_{\text{IRC}}} \right\rceil T_{\text{s}} \ . \tag{11}$$

Since the presented IRC scheme is adaptive, the total time required for IRC T'_{IRC} depends on different events. For the improved IRC scheme, the received signals are exchanged among the relays for signal combining and re-decoding if E_2 occurs. Subsequently, the CRC bits are exchanged again, resulting in 3 sub-events

$$\mathrm{E}_4 = \mathrm{E}_2 \cap (\mathrm{E}_2 \to \mathrm{E}_1) \tag{12a}$$

$$\mathrm{E}_5 = \mathrm{E}_2 \cap (\mathrm{E}_2 \to \mathrm{E}_2) \tag{12b}$$

$$\mathrm{E}_6 = \mathrm{E}_2 \cap (\mathrm{E}_2 \to \mathrm{E}_3) \ , \tag{12c}$$

where $\mathrm{E}_2 \to \mathrm{E}_i$ represents the event that after exchanging the received signals and re-decoding, E_2 turns to E_i. Noticeably, if $\mathrm{E}_2 \to \mathrm{E}_3$ occurs, i.e., at least one but not all relays are correct after received signal exchange, the punctured bits are further exchanged since it is an efficient scheme [1]. Depending on the different events, T'_{IRC} is given by

$$T'_{\text{IRC}} = \begin{cases} KT_{\text{s}} & \text{if } \mathrm{E}_1 \\ (2K - |\mathcal{D}|)\, T_{\text{s}} + T_{\text{pun}} & \text{if } \mathrm{E}_3 \\ 2KT_{\text{s}} + T_{\text{rec}} & \text{if } \mathrm{E}_4,\ \mathrm{E}_5 \\ (3K - |\mathcal{D}''|)\, T_{\text{s}} + T_{\text{rec}} + T_{\text{pun}} & \text{if } \mathrm{E}_6 \ . \end{cases} \tag{13}$$

Here $\mathcal{D}''$ represents the set containing all correct relays after the received signal exchange. Note that each relay requires one individual symbol duration T_{s} to broadcast its CRC bit, resulting in KT_{s} to determine the set $\mathcal{D}$ in the VAA. In contrast, only the erroneous relays have to update and send their decoding status after re-decoding. T_{rec} is involved in $\mathrm{E}_2 = \mathrm{E}_4 \cup \mathrm{E}_5 \cup \mathrm{E}_6$. T_{pun} shows up in E_6 since the punctured bits are also exchanged in this case.

In order to achieve a fair comparison between the scheme without IRC, the IRC scheme presented in [6] and the improved IRC scheme in this paper, the throughput of the overall system is analyzed taking into account the extra time consumption T'_{IRC}. Since T'_{IRC} depends on the different events, the averaged throughput of the overall system η for the improved IRC scheme is calculated by

$$\eta = \sum_{\substack{i=1 \\ i \neq 2}}^{6} \Pr\{\mathrm{E}_i\} \, \frac{N_{\text{FFT}} \log_2 M \, R_{\text{C}}}{2T_{\text{OFDM}} + T_{\text{IRC},i}} \left(1 - \text{FER}_{\text{D}}\right) \ , \tag{14}$$

where $\Pr\{\mathrm{E}_i\}$ and $T_{\text{IRC},i}$ denote the event probability and the time duration for IRC in case that E_i occurs, respectively. The frame error rate (FER) at the destination is denoted as FER_{D}. Note that both $\Pr\{\mathrm{E}_i\}$ and FER_{D} can be achieved by simulations. The throughput η defined in (14) represents the number of correct information bits received at D per unit time such that it captures the impact of the extended time duration T'_{IRC} in case of IRC.

[1] It was shown in [6] that when all punctured bits are exchanged from one of the correct relays, all erroneous relays will be re-decoded correctly in our system setup.

V. Energy Model

The throughput analysis presented in Subsection IV-E takes into account the extra time consumption for IRC. However, IRC requires also additional energy cost. For practical preferences, we analyze the total energy consumption for signal transmission, baseband processing and RF circuit at all relays. To this end, an energy model is constructed in [6] for a fair comparison between different schemes, which is shortly reviewed in the sequel.

Denoting $\mathcal{E}_{\text{relay}}$ the total energy consumption at all relays during transmitting one OFDM frame from S to D via VAA, $\mathcal{E}_{\text{relay}}$ can be divided into the energy required to support the source-relay-destination transmission $\mathcal{E}_{\text{SRD}}$ and the energy dedicated to IRC $\mathcal{E}_{\text{IRC}}$. This yields

$$\mathcal{E}_{\text{relay}} = \mathcal{E}_{\text{SRD}} + \mathcal{E}_{\text{IRC}} \ , \tag{15}$$

which can be further decomposed into the RF circuit, baseband processing and signal transmission energy

$$\mathcal{E}_{\text{SRD}} = \mathcal{E}_{\text{SRD,RF}} + \mathcal{E}_{\text{SRD,Base}} + \mathcal{E}_{\text{SRD,Signal}} \tag{16a}$$

$$\mathcal{E}_{\text{IRC}} = \mathcal{E}_{\text{IRC,RF}} + \mathcal{E}_{\text{IRC,Base}} + \mathcal{E}_{\text{IRC,Signal}} \ . \tag{16b}$$

The energy consumption for each component has been discussed in detail in [6]. Note that the improved IRC scheme based on received signal exchange leads to a variant formulation of the energy consumption $\mathcal{E}_{\text{IRC}}$ for IRC compared to the original scheme. Furthermore, $\mathcal{E}_{\text{IRC,Signal}}$ can be ignored as shown in [6]. Therefore, only the two components $\mathcal{E}_{\text{IRC,RF}}$ and $\mathcal{E}_{\text{IRC,Base}}$ need to be re-evaluated.

A. RF Circuit Energy for IRC

In order to evaluate the RF energy consumption for IRC $\mathcal{E}_{\text{IRC,RF}}$, the overhead for exchanging the CRC bits is neglected in order to simplify the analysis. Since the circuit power of most RF parts is generally assumed to be fixed, the power consumption in one transmitter $\mathcal{P}_{\text{Tx}}$ and one receiver $\mathcal{P}_{\text{Rx}}$ is the summation of the fixed components, such as mixer, LNA and IFA [10]. Note that when the received signals are exchanged among the relays as shown in Section IV, it is always the case that one relay transmits and $(K-1)$ relays receive. This leads to the RF energy consumption for the received signal exchange

$$\mathcal{E}_{\text{IRC,RF,rec}} = (\mathcal{P}_{\text{Tx}} + (K-1)\mathcal{P}_{\text{Rx}}) \cdot T_{\text{rec}} \ . \tag{17}$$

In contrast, the RF energy consumed for the punctured bits exchange scheme in Section III is calculated as

$$\mathcal{E}_{\text{IRC,RF,pun}} = (\mathcal{P}_{\text{Tx}} + (K - |\mathcal{D}^*|)\, \mathcal{P}_{\text{Rx}}) \cdot T_{\text{pun}} \tag{18}$$

because only the erroneous relays need to receive the punctured bits. Here $\mathcal{D}^* = \mathcal{D}$ for E_3 and $\mathcal{D}^* = \mathcal{D}''$ for E_6. Consequently, the RF energy consumption for IRC $\mathcal{E}_{\text{IRC,RF}}$ of the improved scheme is calculated by averaging $\mathcal{E}_{\text{IRC,RF,pun}}$ and $\mathcal{E}_{\text{IRC,RF,rec}}$ depending on the involved events

$$\begin{aligned} \mathcal{E}_{\text{IRC,RF}} = {} & \left(\Pr\{\mathrm{E}_3\} + \Pr\{\mathrm{E}_6\}\right) \mathcal{E}_{\text{IRC,RF,pun}} \\ & + \Pr\{\mathrm{E}_2\}\, \mathcal{E}_{\text{IRC,RF,rec}} \ . \end{aligned} \tag{19}$$

B. Baseband Processing Energy for IRC

The energy consumption for baseband processing is calculated at CMOS level, where one CMOS gate consumes dynamic energy (switching power and short-circuit current) and static energy (subthreshold leakage current, gate leakage current, etc.). It was shown in [11] that the dominating term in a "well-designed" circuit is the switching component. To this end, the static energy consumption is neglected in this paper and the energy for one CMOS gate consists of only the dynamic part given by

$$\mathcal{E}_{\text{CMOS}} = \beta C_{\text{L}} V_{\text{dd}}^2 \ . \tag{20}$$

Here C_{L} represents the load capacity of one CMOS gate, $0 \leq \beta \leq 1$ is the effective switching factor and V_{dd} denotes the supply voltage. Based on this energy model for one CMOS, the baseband processing energy for IRC $\mathcal{E}_{\text{IRC,base}}$ is calculated by counting the number of involved CMOS gates N_{IRC} in the IRC phase, such that

$$\mathcal{E}_{\text{IRC,base}} = N_{\text{IRC}} \mathcal{E}_{\text{CMOS}} \ . \tag{21}$$

The baseband energy captures the FFT, IFFT, interleaver, de-interleaver, memory units and the decoding block using the Viterbi algorithm. For example, the number of CMOS gates used for a 16-bit FFT and Viterbi decoder is around 4.2×10^6 and 0.45×10^6, respectively [6]. Compared to the original IRC scheme, the improved scheme requires additionally $K(K-1)$ FFTs to obtain the channel coefficients in frequency domain for the CSI exchange. Furthermore, K times decoding efforts are required for re-decoding at all relays when the received signals are exchanged in E_2.

VI. Performance Evaluation

A. Parameter Settings

A distributed relaying system with $K = 4$ relays using DF is considered. The constituted VAA joints the direct line between the source S and the destination D with $d_{\text{SR}} = d_{\text{RD}}$. The relaying channels for the SR and the RD links are assumed to be block Rayleigh fading with path-loss exponent $\alpha = 3.5$ and $N_{\text{H}} = 5$ multi-path taps. The channel coefficients are assumed to be invariant during $L = 10$ OFDM frames. We consider an equal power allocation between S and the VAA, i.e., $\mathcal{P}_{\text{S}} = \mathcal{P}_{\text{R}}$, and $\mathcal{P}_{\text{R}}$ is equally assigned to the active relays. The bandwidth of all links is set to $W = 1\text{MHz}$, the background noise power density equals $N_0 = -174\text{dBm/Hz}$, and $\sigma_n^2 = N_0 W$ holds. The received SNRs at R and D are defined as $\text{SNR}_{\text{SR}} = \mathcal{P}_{\text{S}} / \left(\sigma_n^2 d_{\text{SR}}^{\alpha}\right)$ and $\text{SNR}_{\text{RD}} = \mathcal{P}_{\text{R}} / \left(\sigma_n^2 d_{\text{RD}}^{\alpha}\right)$, respectively. One OFDM frame occupies $N_{\text{FFT}} = 256$ subcarriers with 16-QAM modulation. IRC is only subject to AWGN disturbance with $\text{SNR}_{\text{IRC}} = 30\text{dB}$ at the receiver side due to closely located relays. 256-QAM modulation is used for the inter-relay communications. The quantization level is set to $Q = 4$ for the received signal exchange with ZF considered before quantization.

Denoting K_{act} the number of active relays transmitting to D, the VAA employs an OSTBC of rate $R_{\text{STBC}} = 3/4$ [12] when $K_{\text{act}} = 3$ or 4 and $R_{\text{STBC}} = 1$ when $K_{\text{act}} = 2$. The relay simply unicasts to the destination when $K_{\text{act}} = 1$. The channel code rate used for the RD link transmission is adapted to $R_{\text{C,RD}} = 2/3$ in case of using the OSTBC of rate $R_{\text{STBC}} = 3/4$ for rate matching. For the schemes with IRC, the source uses a rate-compatible punctured convolutional (RCPC) code [13] with mother code rate $R_{\text{C,mom}} = 1/3$ and generator polynomial $[13, 15, 11]_8$. By puncturing $n_{\text{pun}} = 512$ bits, the effective code rate $R_{\text{C}} = 1/2$ is achieved for transmission. The Viterbi algorithm is used for decoding.

The energy consumption for baseband processing is calculated based on a 90nm CMOS processor [14]. The load capacity is set to $C_{\text{L}} = 1\text{fF}$ and the effective switching factor equals $\beta = 12.5\%$.

B. Simulation Results

For a distributed relaying system considering the improved IRC scheme, the event probabilities for the number of correct relays before re-decoding $|\mathcal{D}|$ and after re-decoding $|\mathcal{D}'|$ are drawn in Fig. 7. It can be observed in a), that event E_2 ($|\mathcal{D}| = 0$) occurs more likely in the low SNR region, where the received signals are exchanged more frequently. Note that E_3 is the superposition of $|\mathcal{D}| \in \{1, 2, 3\}$ and occurs more likely at medium SNR, indicating that the punctured bits exchange takes place more frequently in this region. Fig. 7b) shows the event probabilities for the number of correct relays $|\mathcal{D}'|$ after IRC and re-decoding. The presented IRC scheme in [6] is shown as reference, where no information is exchanged in E_2, such that the corresponding curve for $|\mathcal{D}'| = 0$ remains unchanged. Furthermore, the curves for 1, 2 and 3 correct relays after re-decoding totally vanish in case that all punctured bits $n_{\text{IRC}} = 512$ are exchanged. For the improved IRC scheme presented in this paper, part of or the whole received OFDM frame are exchanged among the relays when E_2 occurs, which may result in correct relays after re-decoding based on signal combining. Therefore, the probability for all relays being erroneous after re-decoding gets smaller, as can be observed in Fig. 7b). It is also shown that exchanging larger amount of the received signals leads to improved re-decoding quality at the relays, as comparing the improved IRC schemes using full exchange and partial exchange of received signals with different λ.

Fig. 8 shows the throughput performance of the overall system for the improved IRC scheme using full exchange and partial exchange of received signals compared to the scheme without IRC and the reference scheme in [6]. It can be observed that exchanging received signals when all relays are erroneous further improves the throughput in general, especially in the low SNR region. Note that due to the large amount of overhead, using full exchange of received signals becomes even worse than the existing IRC scheme in [6] as SNR_{SR} increases. The improved IRC scheme by applying partial exchange of received signals with $\lambda = 1$ shows superior throughput performance in our system setup considering only the transmit power. However, the benefit of choosing a smaller λ, e.g., $\lambda = 1/4$ may lead to improved performance when the

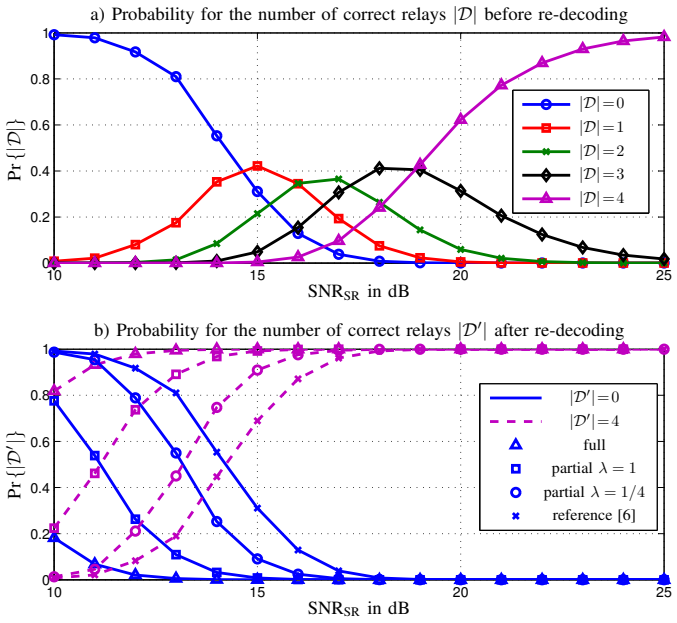

Fig. 7. Event probabilities for different number of correct relays before re-decoding a) and after re-decoding b) using the improved IRC scheme. In E_3 $n_{\mathrm{IRC}} = 512$ punctured bits are exchanged.

energy consumption for baseband processing and RF circuit is also taken into account, as discussed in the sequel.

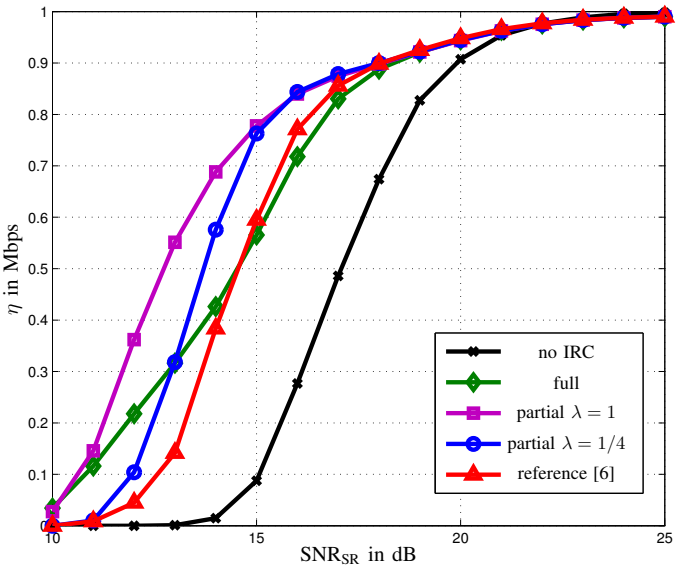

Fig. 8. System throughput η in (14) versus $\mathrm{SNR}_{\mathrm{SR}}$ for the improved IRC scheme using full exchange and partial exchange, $d_{\mathrm{SD}} = 500\,\mathrm{m}$. All punctured bits $n_{\mathrm{IRC}} = 512$ are exchanged in E_3.

Subsequently, the energy consumption for baseband processing $\mathcal{E}_{\mathrm{Base}} = \mathcal{E}_{\mathrm{SRD,Base}} + \mathcal{E}_{\mathrm{IRC,Base}}$ and RF circuit $\mathcal{E}_{\mathrm{RF}} = \mathcal{E}_{\mathrm{SRD,RF}} + \mathcal{E}_{\mathrm{IRC,RF}}$ is drawn in Fig. 9. As can be observed, the baseband and RF circuit energy depends on $\mathrm{SNR}_{\mathrm{SR}}$, which decreases with growing $\mathrm{SNR}_{\mathrm{SR}}$. This is because the exchange of received signals and punctured bits for IRC takes place more frequently at low $\mathrm{SNR}_{\mathrm{SR}}$ and medium at $\mathrm{SNR}_{\mathrm{SR}}$, respectively. However, IRC is rarely required at high $\mathrm{SNR}_{\mathrm{SR}}$. Note that full exchange of received signals consumes much more baseband and RF circuit energy due to large amount of exchanged received signals. Furthermore, partial exchange of received signals with smaller λ results in less energy consumption, as shown in Fig. 9.

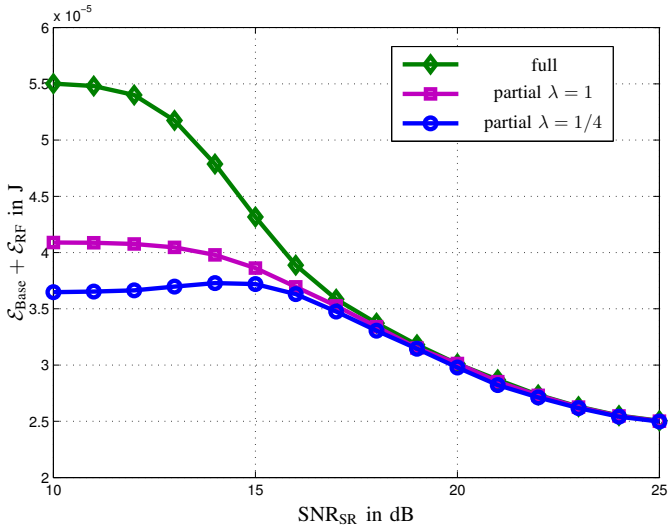

Fig. 9. Energy consumption for baseband processing and RF circuit $\mathcal{E}_{\mathrm{Base}} + \mathcal{E}_{\mathrm{RF}}$ at all relays for full exchange and partial exchange of received signals.

The Pie chart of the energy proportions in (16) for the improved IRC scheme using full exchange of received signals with $\mathrm{SNR}_{\mathrm{SR}} = 14\,\mathrm{dB}$ is shown on the left side of Fig. 10 as an example. The SD distance is set to $d_{\mathrm{SD}} = 50\,\mathrm{m}$. Due to small d_{SD}, the baseband and RF circuit energy dominates the total energy consumption $\mathcal{E}_{\mathrm{relay}}$ with negligible transmit energy $\mathcal{E}_{\mathrm{SRD,Signal}}$. On the right side, the corresponding system throughput η in (14) versus the total energy consumption $\mathcal{E}_{\mathrm{relay}}$ for the improved IRC scheme using both full exchange and partial exchange of received signals is plotted. Note that $\mathrm{SNR}_{\mathrm{SR}}$ increases upwards with the adjacent markers corresponding to a 1 dB step on each curve. Furthermore, both η and $\mathcal{E}_{\mathrm{relay}}$ depend on $\mathrm{SNR}_{\mathrm{SR}}$, as shown by Fig. 8 and 9, respectively. With growing $\mathrm{SNR}_{\mathrm{SR}}$, the throughput η increases but the total energy consumption $\mathcal{E}_{\mathrm{relay}}$ decreases because the transmit energy is negligible. Therefore, the throughput even increases with less energy consumption for small d_{SD}, as shown in Fig. 10. Additionally, it can also be observed that for $d_{\mathrm{SD}} = 50\,\mathrm{m}$ partial exchange of received signals with a smaller λ, e.g., $\lambda = 1/4$, achieves better performance compared to $\lambda = 1$ since less overhead results in reduced baseband and RF circuit energy consumption, according to Fig. 9.

When the SD distance d_{SD} grows larger, the transmit energy can not be neglected any more compared to the baseband and RF circuit energy, as shown by the Pie chart for the energy proportions in Fig. 11 for $d_{\mathrm{SD}} = 150\,\mathrm{m}$. In this case, the throughput increases monotonically with $\mathcal{E}_{\mathrm{relay}}$. Note

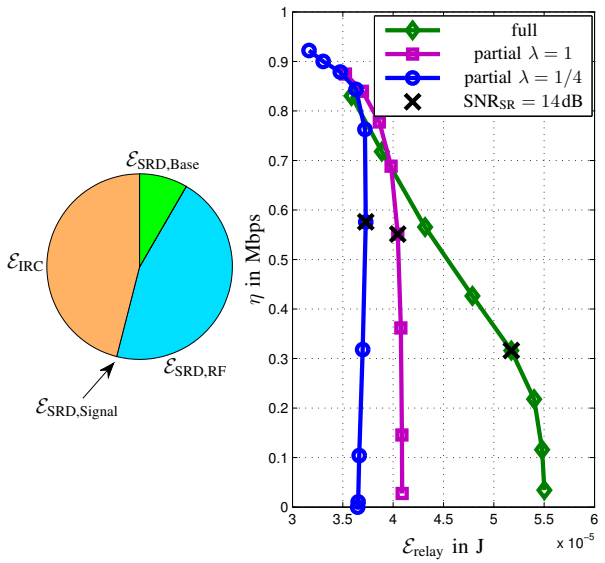

Fig. 10. Throughput performance versus $\mathcal{E}_{\text{relay}}$ for $d_{\text{SD}} = 50\,\text{m}$. The Pie chart shows the energy proportions in (16) for the improved IRC scheme using full exchange of received signals with $\text{SNR}_{\text{SR}} = 14\,\text{dB}$.

that partial exchange of received signals still provides better throughput performance than full exchange even in the low SNR region. In contrast, for large SD distance, e.g., $d_{\text{SD}} = 500$ m, the transmit energy dominates the total energy consumption with negligible baseband and RF circuit energy, full exchange outperforms partial exchange with $\lambda = 1/4$ at low SNR_{SR}, as presented in Fig. 8. This leads to the conclusion, that with respect to the total energy consumption, the amount of exchanged received signals for the improved IRC scheme needs to be chosen appropriately depending on the distance.

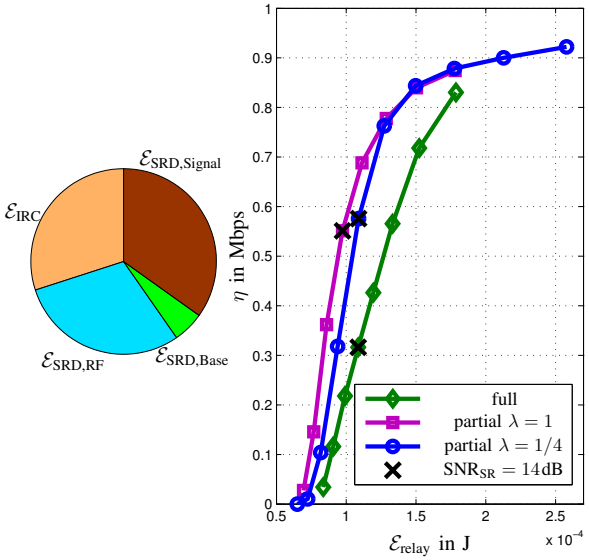

Fig. 11. Throughput performance versus $\mathcal{E}_{\text{relay}}$ for $d_{\text{SD}} = 150\,\text{m}$. The Pie chart shows the energy proportions in (16) for the improved IRC scheme using full exchange of received signals with $\text{SNR}_{\text{SR}} = 14\,\text{dB}$.

VII. Conclusion

In this paper we presented an improved inter-relay cooperation (IRC) scheme for a distributed relaying network using OSTBC. In addition to exchanging punctured bits if at least one but not all relays are error-free, the whole or part of the received OFDM frame are exchanged among the relays in the VAA when all relays fail to decode the source message correctly. Based on the exchanged received signals, full exchange and partial exchange of received signals have been investigated and evaluated using a throughput analysis. In order to achieve a fair comparison, the total energy consumption for signal transmission, baseband processing and RF circuit is evaluated based on an energy model at all relays. Simulation results show the superior performance by using the improved IRC scheme under proper amount of exchanged received signals.

VIII. Acknowledgement

This work was supported in part by the German Research Foundation (DFG) under grant Wu 499/7 and Pa 438/4 within the priority program "Communication in Interference Limited Networks (COIN)", SPP 1397.

References

[1] J. N. Laneman, D. N. C. Tse, and G. W. Wornell, "Cooperative Diversity in Wireless Networks: Efficient Protocols and Outage Behavior," *IEEE Transactions on Information Theory*, vol. 50, no. 12, pp. 3062–3080, Dec. 2004.

[2] J. N. Laneman and G. W. Wornell, "Distributed Space-Time-Coded Protocols for Exploiting Cooperative Diversity in Wireless Networks," *IEEE Transactions on Information Theory*, vol. 49, no. 10, pp. 2415–2425, Oct. 2003.

[3] Q. Huang, M. Ghogho, J. Wei, and P. Ciblat, "Timing and Frequency Synchronization for OFDM based Cooperative Systems," in *IEEE International Conference on Acoustics, Speech and Signal Processing (ICASSP'09)*, Taipei, Taiwan, Apr. 2009.

[4] R. Tannious and A. Nosratinia, "Spectrally-Efficient Relay Selection with Limited Feedback," *IEEE Journal on Selected Areas in Communications*, vol. 26, no. 8, pp. 1419–1428, Oct. 2008.

[5] A. Tajer and A. Nosratinia, "Opportunistic Cooperation via Relay Selection with Minimal Information Exchange," in *IEEE International Symposium on Information Theory (ISIT'07)*, Nice, France, Jun. 2007.

[6] M. Wu, W. Xue, D. Wübben, A. Dekorsy, and S. Paul, "Energy-aware Design of Inter-Relay Cooperation for Distributed Relaying Networks," in *8th International Symposium on Wireless Communication Systems (ISWCS'11)*, Aachen, Germany, Nov. 2011.

[7] L. Yue, "Analysis of Generalized Selection Combining Techniques," in *IEEE 51st Vehicular Technology Conference (VTC'00-Spring)*, Tokyo, Japan, May 2000.

[8] S. W. Kim, Y. G. Kim, and M. K. Simon, "Generalized Selection Combining based on the Log-Likelihood Ratio," *IEEE Transactions on Communications*, vol. 52, no. 4, pp. 521–524, Apr. 2004.

[9] J. G. Proakis, *Digital Communications*, McGraw-Hill, 4th edition, 2000.

[10] S. Cui, A. J. Goldsmith, and A. Bahai, "Energy-Constrained Modulation Optimization for Coded Systems," in *IEEE Global Telecommunications Conference (GLOBECOM'03)*, San Francisco, USA, Dec. 2003.

[11] A. P. Chandrakasan, S. Sheng, and R. W. Brodersen, "Low-power CMOS Digital Design," *IEEE Journal of Solid-State Circuits*, vol. 27, no. 4, pp. 473–484, Apr. 1992.

[12] V. Tarokh, H. Jafarkhani, and A. R. Calderbank, "Space-Time Block Codes from Orthogonal Designs," *IEEE Transactions on Information Theory*, vol. 45, no. 5, pp. 1456–1467, Jul. 1999.

[13] J. Hagenauer, "Rate-Compatible Punctured Convolutional Codes (RCPC Codes) and their Applications," *IEEE Transactions on Communications*, vol. 36, no. 4, pp. 389–400, Apr. 1988.

[14] E. Sicard and S. D. Bendhia, *Advanced CMOS Cell Design*, McGraw-Hill Professional, 2007.